On the dynamic readout of sub-diffraction-limit pit arrays with a silver thin film

2007 J. Phys.: Condens. Matter 19 276208

(http://iopscience.iop.org/0953-8984/19/27/276208)

IOP Publishing Journal of Physics: Condensed Matter

J. Phys.: Condens. Matter **19** (2007) 276208 (11pp) doi:10.1088/0953-8984/19/27/276208

On the dynamic readout of sub-diffraction-limit pit arrays with a silver thin film

Jingsong Wei[1,2] and Mufei Xiao[2]

[1] Shanghai Institute of Optics and Fine Mechanics, Chinese Academy of Sciences, Shanghai 201800, People's Republic of China
[2] Centro de Ciencias de la Materia Condensada Universidad Nacional Autónoma de Mexico, Apartado Postal 2681, CP 22800 Ensenada, Baja California, Mexico

E-mail: weijingsong@siom.ac.cn and mufei@ccmc.unam.mx

Received 17 February 2007, in final form 27 April 2007
Published 21 June 2007
Online at stacks.iop.org/JPhysCM/19/276208

Abstract
Fast moving arrays of periodic sub-diffraction-limit pits were dynamically read out via a silver thin film. The mechanism of the dynamic readout is analysed and discussed in detail, both experimentally and theoretically. The analysis and experiment show that, in the course of readout, surface plasmons can be excited at the silver/air interface by the focused laser beam and amplified by the silver thin film. The surface plasmons are transmitted into the substrate/silver interface with a large enhancement. The surface waves at the substrate/silver interface are scattered by the sinusoidal pits of sub-diffraction-limit size. The scattered waves are collected by a converging lens and guided into the detector for the readout.

(Some figures in this article are in colour only in the electronic version)

1. Introduction

Recently, there has been growing research interest in sub-diffraction imaging with the so-called silver superlens, which is essentially a flat silver thin film [1–9].

For an optical device involving noble-metal surfaces, one often pays great attention to the possible role of the surface plasmon, which can be excited and propagates laterally within a limited distance at the metal/dielectric interfaces [10]. In the normal direction, the surface plasmons are evanescent fields that extend exponentially into both the air or dielectric side (with a tail comparable to the wavelength of the light) and the metal side (with a much shorter tail due to absorption in the metal). However, for ultrathin metallic films where the dielectric function is negative, the film may amplify the evanescent field from one interface to another, which has been documented extensively in the past (see, for instance, [10]).

The recent development of the superlens stemmed, however, from a different context, namely the left-handed medium. In 1968, Veselago [11] first predicted that a flat slab of left-handed material that bears a negative refractive index could focus electromagnetic waves, in the same way as a curved optical lens. In 2000, Pendry [1] pointed out theoretically that the negative refraction could make a perfect lens that refocuses all Fourier components of a point source, including the evanescent waves. He also estimated that the perfect lens could be made of a silver slab with a negative dielectric function, which is herewith referred to as the silver superlens. Following Pendry's predictions, Zhao *et al* [3, 4] found experimentally that evanescent waves could be regenerated and rapidly amplified via a silver superlens. Using the silver superlens, Fang *et al* [5, 6] demonstrated sub-diffraction-limit imaging with a 60 nm half-pitch resolution and, independently, Melville *et al* [7–9] reported submicron optical lithography with features as small as 250 nm.

Up to now, the silver superlens has found a few useful applications in optics. Among others, one of us (JW) and colleagues reported in 2005 the dynamic readout of sub-diffraction-limit pit arrays in the far-field [12], which was shown to be useful for ultrahigh-density optical storage [13, 14]. It is interesting to note that, in the experiments conducted by others [5–9], light sources of wavelength 360 nm were used, which is close to the plasmon frequency of silver. However, in our experiments, the wavelength of the readout laser was 780 nm, which is far away from the plasmon resonance of silver. Therefore, the detailed readout mechanism has yet to be explored.

In order to understand the observed phenomena in our previous experiments and to develop further the application of a superlens in ultrahigh-density optical recording, in the present paper we report some detailed experimental and theoretical analyses, as well as discussions about the dynamic readout mechanism.

We start with a general discussion on the nature of the silver superlens as well as its relationship with left-handed focusing, and a qualitative deduction of the main paths involved in the sub-diffraction-limit readout. We then concentrate the analysis on the specific application of the dynamic readout of sub-diffraction-limit pit arrays. We present the experimental procedures and results. Following the experimental results, we present a theoretical study on the device, including the establishment and amplification of the surface plasmons inside the silver thin film. The amplification of the surface plasmon waves is confirmed experimentally. Finally, on the basis of the experimental and theoretical analyses, we draw conclusions on the mechanism of the dynamic readout of the sub-diffraction-limit pit arrays by a silver thin film.

The rest of the paper is organized as follows. In section 2, general discussions about the nature of the silver superlens and the relationship between the device and the left-handed focusing are presented. In section 3, experimental procedures and results are shown on super-resolution with silver thin films. In section 4, the production of surface plasmons on interfaces is explored. In section 5, the amplification of the surface plasmon is studied both theoretically and experimentally. Finally, the work is concluded in section 6.

2. Thin silver film and superlens

In this section we discuss the nature of the silver superlens and its role in the readout mechanism. Let us start with the left-handed focusing predicted by Veselago in 1968 [11]. The idea was that a flat plate of left-handed material would refocus a point light source the same way as a curved optical lens. The principle behind the prediction is that the material has to be left-handed, meaning that the electric and magnetic fields and the wave vector form a left-handed system and, consequently, the refractive index of the material becomes negative. Therefore, the refractive beam goes in the opposite direction [11]. In other words, the left-handed plate acts as a curved lens and is able to focus the light at one point on the other side of the plate.

It is well known that light focusing has a fundamental limit on the size of the focus point due to the diffraction of light. The diffraction limit is related to the light wavelength as $\sim\lambda/2$, which in turn restricts the resolution of imaging. However, the diffraction limit applies only to the propagating waves and has no effects on the evanescent field. Any light source contains both propagating and evanescent components. Conventional optics collect only the propagating components, and thus are subject to the diffraction limit, whereas the evanescent components are limited by the point source within near-field distances, which are much shorter than the wavelength [17]. Should the evanescent components be collected by a special lens along with the propagating components, the focused spot would no longer be limited by diffraction. Therefore, such a special lens may be called a perfect lens. In 2000, Pendry [1] pointed out theoretically that negative refraction could make a perfect lens that focuses all Fourier components of a point source, including the evanescent waves. The reason is that the evanescent components may be amplified within the left-handed material. Since the publication of [1], there have been some further discussions on the perfect lens [15, 16]. The discussion has been concentrated mainly on two issues, namely (1) if the evanescent field is actually amplified in the left-handed material [15] and (2) if the evanescent fields can be really focused [16]. In the present work, we shall, however, refrain from taking part in the above discussion on the perfect lens of left-handed material.

Instead, we concentrate on whether a silver thin film can be an alternative for the left-handed perfect lens, and specifically how the film can help to read out sub-diffraction-limit details. The possibility of using a thin silver film as a perfect lens has been predicted and tested recently [1–9]. Since a left-handed material does not exist in nature and can hardly be fabricated for visible light, one is tempted to believe that a silver film would be an alternative, as silver is usually nonmagnetic and has a dominant negative dielectric permittivity in visible [1, 2].

The unique condition for a material to be left-handed is for it to have a negative refractive index, which usually requires that the relative electrical permittivity, ϵ, and magnetic permeability, μ, are simultaneously negative [11]. Therefore, as far as the handedness of the material is concerned, the silver in visible light remains right-handed, no matter how weak the magnetic reaction is. In other words, a flat silver thin film cannot be a lens within the framework of linear optics[3].

However, the other characteristic of a perfect lens can be fulfilled for the silver thin film, namely amplification of the evanescent fields. Indeed, it has been well known for quite a long time that surface plasmons can be excited and that they propagate laterally within a limited distance at metal/dielectric interfaces [10]. In the normal direction, the surface plasmons are evanescent fields that extend exponentially into both the air or dielectric side (with a tail comparable to the wavelength of light) and the metal side (with a much shorter tail due to absorption in the metal). However, for ultrathin metallic films where the dielectric function is negative [19], the film may amplify the evanescent field from one interface to another, which has been documented extensively in the past (see, for instance, [10, 20]).

It becomes clear now that a silver thin film cannot be a perfect lens because, while it is perfect, as it does amplify evanescent fields, it is however not a lens, as it has no negative refraction. The question remaining to be answered is the origin of the sub-diffraction-limit resolution obtained with a silver thin film [3–9, 12]. Our understanding is that the super-resolution could be attributed to the well-known fact that the surface plasmon polaritons on the silver surface have a spatial wavelength in the lateral direction shorter than the light

[3] In nonlinear optics, strong Kerr materials may, however, generate self-imaging effects; see, for instance, [18].

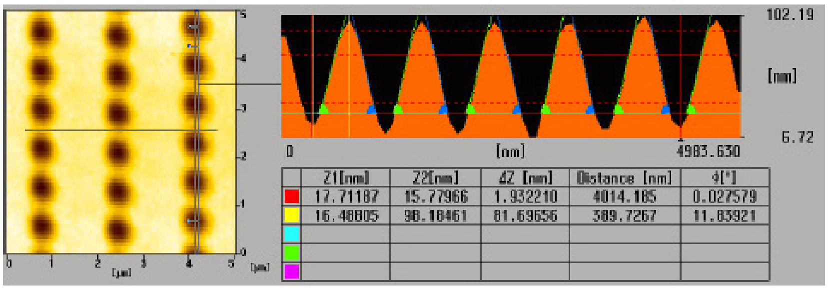

Figure 1. AFM analysis of pit arrays on the disk substrate.

wavelength, plus the fact that the surface plasmon polaritons are strongly enhanced at the interface. Therefore, the features at the interface are actually illuminated by strong surface waves with a shorter wavelength, and therefore can be observed by far-field optics with sub-diffraction-limit resolution. In short, the sub-diffraction-limit resolution is due to the diminished diffraction limit of the surface plasmon polaritons. The above phenomenon has actually been noticed in the past, though in somewhat different contexts and configurations. For example, in [21], sub-diffraction-limit resolution was achieved with far-field optics via two counter-propagating surface plasmons. The two plasmons produce a strong interference pattern, with a spatial wavelength that is much shortened.

The device that we study in the present work has similar characteristics. Periodic arrays of sub-diffraction-limit pits are created at the silver surface that generate surface wave patterns with a shortened spatial wavelength. The film also enables the surface waves to be amplified with a large enhancement.

So far, we have reached a general and deductive explanation for the sub-diffraction-limit resolution obtained via a thin silver film. In the following three sections we shall apply the theory to the dynamic readout of arrays of sub-diffraction-limit pits via a thin silver film. In next section the configuration of the experimental device and the procedure for the experiments will be explained in details. Also, the experimental results are used to demonstrate the key steps in the readout, such as the excitation and amplification of the surface plasmons. After the experimental parts, in the subsequent two sections we give a mathematical evolution along the same steps.

3. Experiments and results

We have conducted some experiments to test the readout mechanism. The experimental procedures and parameters are as follows. The substrate is an optical disk whose refractive index is $n_s = 1.5$ in visible light. There are arrays of pits on the substrate. We used atomic force microscopy (AFM) to look at the size and shape of the pits. Figure 1 shows the AFM morphology of the pit arrays on the optical disk substrates. One finds from figure 1 that the pit depth and diameter (space) are about 50 nm and 389 nm, respectively. The corresponding pitch of the pit trains is about 778 nm. The pit train boundary appears to be of sinusoidal profile.

A silver thin film was deposited directly on the substrate using the dc sputtering method. The dynamic readout setup is composed of a laser of wavelength $\lambda_0 = 780$ and a pickup lens with a numerical apertureof NA $= 0.45$ (see details in [12]). The overall experimental schematic is described in figure 2, including the substrate, the silver coat, and the illuminating and reading lens. The diameter of the focused spot on the silver thin film can be estimated

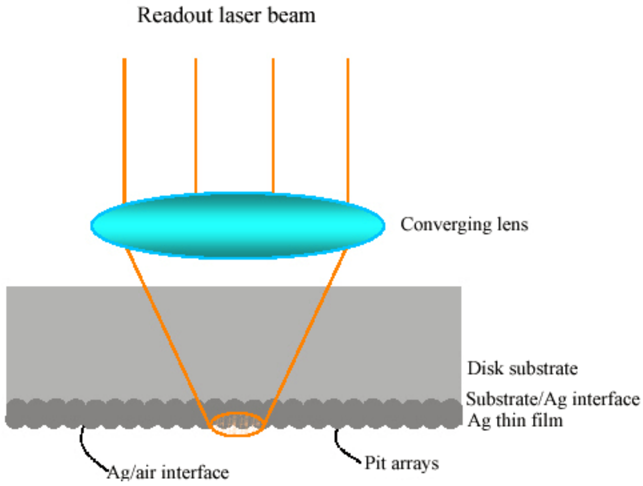

Figure 2. Optical disk structure and dynamic readout schematic of pit trains.

using the diffraction limit $D = 1.22\lambda_0/\mathrm{NA}$ and is $D = 2.115$ μm, which is much larger than the pit size ($\approx$389 nm). The dynamic readout resolution limit can be calculated approximately from $D/4$ and is about 530 nm, so the pit size is smaller than the readout resolution limit and cannot be read out dynamically by conventional read-only optical disk techniques, as was demonstrated in [14].

The situation changes, thanks to the silver thin-film coating. The measured results are shown in figure 3, with the spectral analysis and the RF waveform for pit trains on the optical disk. The carrier-to-noise ratio is about 25 dB, and the RF waveform is modulated into a sinusoidal signal by the pit arrays. The results indicate that the below-diffraction pits can be read out dynamically via the silver thin film, and the silver thin film works as a reflective layer with super-resolution capability. More detailed experimental procedures and results can be found in [12]. Here, we mainly analyse and discuss the dynamic readout mechanism and the role of the silver thin film.

4. Surface plasmon excitation

In our experiments, the silver thin film was deposited directly on a substrate with mastered pit arrays. The readout laser beam was first focused on the interface between the substrate and the silver film. The silver film was also modulated into a sinusoidal morphology profile by the pit trains, and can be considered to be a one-dimensional grating on the spot (as shown in figure 2). The interface morphology profile can be described approximately as

$$s(x) = h\sin(k_{\mathrm{g}}, x) \qquad (1)$$

where h represents the pit amplitude, and the spatial wavenumber

$$k_{\mathrm{g}} = \frac{2\pi}{g} \qquad (2)$$

where the spatial wavelength g represents the pitch of the pit arrays; in our experiment, $g = 778$ nm.

As we know, surface plasmons are electron oscillations near an interface (or surface) and can be excited when translational invariance is broken in the direction perpendicular to the

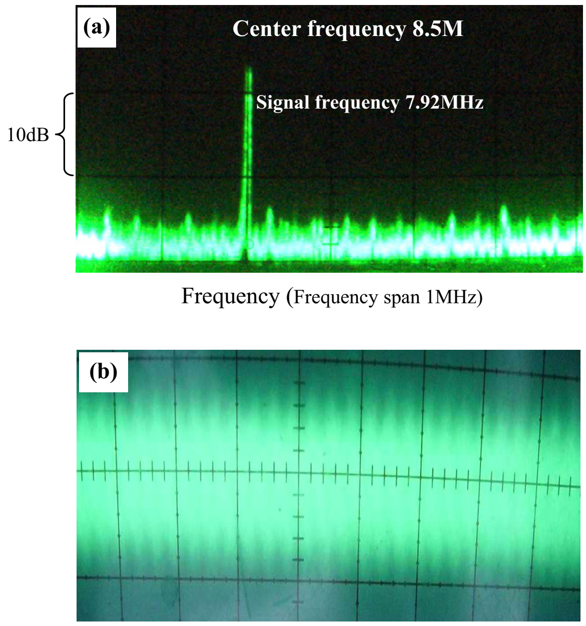

Figure 3. Dynamic readout signal of pit trains from the substrate side (linear velocity 6 m s^{-1}): (a) spectral analysis; (b) RF waveform.

interface (or surface). Therefore, in order to produce the surface plasmons, we need to have a dielectric layer with a positive permittivity and an adjacent metallic (or alloy) layer with a negative permittivity (as shown in figure 4(a)). In our experiments, the surface plasmons may be generated at both the substrate/silver interface and the silver/air interface, because the permittivities of the silver and the substrate (air) are negative and positive, respectively. The dielectric constant for the substrate is $\epsilon_s = 2.25$, for air it is $\epsilon_{air} = 1$, and for silver it is $\epsilon_m = -25 + i1.45$ at a wavelength of 780 nm [19]. The wavevector of the surface plasmons can be calculated using the following formula [10]:

$$k_{sp} = k_0 \sqrt{\frac{\epsilon_m \epsilon_s}{\epsilon_m + \epsilon_s}} \tag{3}$$

with $k_0 = 2\pi/\lambda_0$. In our experiments, $\lambda_0 = 780$ nm. Note that the above dispersion relation was delivered for the condition of semi-infinite media and used for thin-film analyses (see, for instance, [10]).

From equation (3), one finds that $k_{sp} > k_0$, so the surface plasmon (SP) cannot be driven directly by a light beam striking the interface due to the momentum mismatch $\hbar k_{sp} > \hbar k_0$ (as shown in figure 4(a)). However, in our experiments, the SP can be excited by pit trains with a sinusoidal profile. The pit trains are actually used as a diffraction grating coated with the silver thin film, as is described in figure 2.

Due to the sinusoidal profile characteristic of the substrate/silver film interface, wavevector conservation of the input and output fields along the x direction is no longer valid. This leads to the appearance of a discrete set of diffraction orders. The x component of the wave vector of a given diffraction order can be written using the simple relation

$$k_m = k_x \pm m k_g \tag{4}$$

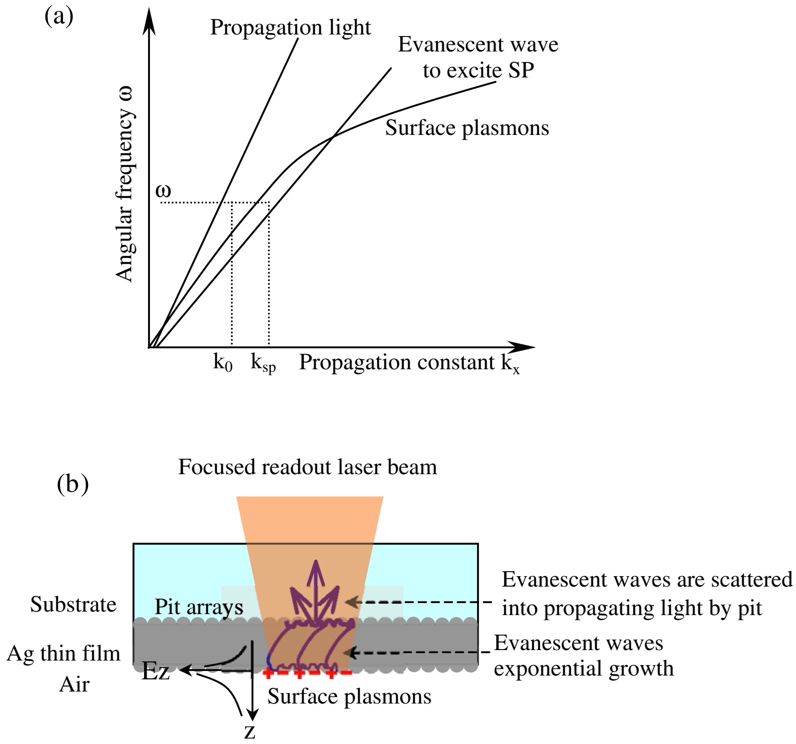

Figure 4. Readout principle with the silver thin film. (a) Dispersion curve for a SP and a photon in free space. (We see the momentum mismatch $\hbar k_{sp} > \hbar k_0$.) (b) Surface plasmon generation, amplification, and scattering and decoupling into propagating light.

with $m = 0, 1, 2, \ldots$ and

$$k_x = k_0 \sin\theta. \tag{5}$$

In order to excite the surface plasmons, the following condition must be fulfilled:

$$k_{sp} = k_m. \tag{6}$$

According to equations (3)–(6), the following formula can be obtained:

$$\theta_{sp}(m) = \sin^{-1}\left[\sqrt{\frac{\epsilon_m \epsilon_s}{\epsilon_m + \epsilon_s}} \mp m\frac{\lambda_0}{g}\right] \tag{7}$$

and in the following, using the formula, we calculate the SP angles at the two interfaces:

(1) At the substrate/silver interface: $\epsilon_s = 2.25$, $\epsilon_m = -25$, $\lambda_0 = 780$ nm, $g = 778$ nm; there exists two solutions, $\theta_{sp}(1) \approx 33°$ and $\theta_{sp}(2) \approx -30°$.
(2) At the silver/air interface: $\epsilon_s = 1$, $\epsilon_m = -25$, $\lambda_0 = 780$ nm, $g = 778$ nm; there exists one solution, $\theta_{sp}(1) = 1.2°$.

The numerical aperture is $\text{NA} = n_{lens} \sin\theta_0 = 0.45$, and the aperture angle of the converging lens is about $\theta_0 < 16.55°$. Comparing θ_{sp} and θ_0, one finds that, for the substrate/silver interface, no surface plasmon is excited, because the required incident angles are not within the numerical aperture of the input lens. However, at the silver/air interface, the surface plasmons can easily be excited by first-order diffraction of the grating due to $\theta_{sp} = 1.2° < 16.55°$.

Therefore, surface plasmons can be excited on the silver/air interface by the first diffraction order from the pit trains, as shown in figure 4(b).

It is well known [10] that a surface plasmon can be excited either by total internal reflection or by a grating structure. The above calculations have proven that in our experiments the surface plasmon can be excited by the grating structure at the silver/air interface. In the following section we show that the excited surface plasmon can be amplified by the thin silver film when the light beam is transmitted back to the substrate side.

5. Surface plasmon amplification

The established surface plasmon has a tail that extends exponentially into the silver film, and the surface plasmon polaritons can propagate along the surface. Since the silver film is thin, the surface plasmon can be transmitted back and enhanced by the film. The transmitted surface plasmon contains the sub-diffraction-limit information of the pit arrays. The scattered wave is collected by the lens for readout. In this section we discuss the field amplification.

Let us analyse the transmission of surface plasmons in the substrate/silver/air structure. Noting that the lateral wavevector of surface waves $k_\parallel = \sqrt{k_x^2 + k_y^2}$ for $k_{zj} = \sqrt{\epsilon_j (\frac{\omega}{c})^2 - k_\parallel^2}$ for $j = 1$ (air), $j = 2$ (Ag) and $j = 3$ (substrate), and that the silver thin film thickness $z = d$, one writes down the overall transmission coefficients for p-polarized light using Fresnel equations as

$$T_{\rm p}(k_\parallel, d) = \frac{(1 + r_{12})(1 + r_{23}) \exp({\rm i}k_{z2}d)}{1 + r_{12}r_{23} \exp(2{\rm i}k_{z2}d)} \qquad (8)$$

where

$$r_{12} = \frac{\frac{k_{z1}}{\epsilon_1} - \frac{k_{z2}}{\epsilon_2}}{\frac{k_{z1}}{\epsilon_1} + \frac{k_{z2}}{\epsilon_2}} \qquad (9)$$

and

$$r_{23} = \frac{\frac{k_{z2}}{\epsilon_2} - \frac{k_{z3}}{\epsilon_3}}{\frac{k_{z2}}{\epsilon_2} + \frac{k_{z3}}{\epsilon_3}}. \qquad (10)$$

In passing, we note that equation (8) also shows that the transmission can be resonantly enhanced if the denominator reaches zero.

For further discussions, we rewrite the expression in equation (8) as

$$T_{\rm p}(k_\parallel, d) = \frac{(1 + r_{12} + r_{23} + r_{12}r_{23}) \exp(-{\rm i}k_{z2}d)}{r_{12}r_{23} + \exp(-2{\rm i}k_{z2}d)}. \qquad (11)$$

One realizes immediately that the denominator in equation (11) now contains two terms, $r_{12}r_{23}$ and $\exp(-2{\rm i}k_{z2}d)$. One further notices that k_{z2} is essentially an imaginary number, and that the term $\exp(-2{\rm i}k_{z2}d)$ is thus a number that increases exponentially with the film thickness d. On the other hand, the first term in the denominator in equation (11), $r_{12}r_{23}$, is usually a large number for metallic interfaces. This can be checked out from the expressions in equations (9) and (10). Inputting the wavenumber from equation (3) into equations (9) and (10), one concludes that both r_{12} and r_{23} become 0 or ∞. The general understanding is that the zero solution corresponds to the s-polarization, whereas the infinite solution is suitable for the p-polarization (see, for instance, the appendix in [22]). In the present situation, we deal with p-polarized fields. Therefore, the term $r_{12}r_{23}$ goes to infinity. For real metals, the term of course becomes a large complex number. Let us go back to discuss the denominator in equation (11). If $r_{12}r_{23} \gg \exp(-2{\rm i}k_{z2}d)$, the second term is negligible. This happens only when the thickness

d is small, which is the case in our experiments. With this condition, one further has $\frac{1}{r_{12}r_{23}} \approx 0$, and the transmission coefficient is approximately

$$T_p(k_\parallel, d) \approx \left(\frac{1}{r_{12}} + \frac{1}{r_{23}} + 1\right) \exp(-ik_{z2}d). \tag{12}$$

Since

$$k_{z2} = \sqrt{\epsilon_2 \left(\frac{\omega}{c}\right)^2 - k_\parallel^2} = i\sqrt{k_\parallel^2 - \epsilon_2 \left(\frac{\omega}{c}\right)^2} \tag{13}$$

one has eventually

$$T_p(k_\parallel, d) \approx \left(\frac{1}{r_{12}} + \frac{1}{r_{23}} + 1\right) \exp\left(d\sqrt{k_\parallel^2 - \epsilon_2 \left(\frac{\omega}{c}\right)^2}\right). \tag{14}$$

Equation (14) indicates that the overall transmission coefficient T_p presents exponential growth if $r_{12}r_{23} \gg \exp(-2ik_{z2}d)$.

Let us now have an estimation for the term $r_{12}r_{23}$ to be a large number, say $r_{12}r_{23} \gg 1$. In the electrostatic limit, $k_{zj} = ik_\parallel$ and, assuming that both the air and the substrate are loss-free, one has

$$\left|\frac{k_{z1}}{\epsilon_1} - \frac{k_{z2}}{\epsilon_2}\right| \left|\frac{k_{z2}}{\epsilon_2} - \frac{k_{z3}}{\epsilon_3}\right| \gg \left|\frac{k_{z1}}{\epsilon_1} + \frac{k_{z2}}{\epsilon_2}\right| \left|\frac{k_{z2}}{\epsilon_2} + \frac{k_{z3}}{\epsilon_3}\right| \tag{15}$$

which equivalently is

$$|\epsilon_2 - \epsilon_1| \, |\epsilon_3 - \epsilon_2| \gg |\epsilon_2 + \epsilon_1| \, |\epsilon_3 + \epsilon_2| \,. \tag{16}$$

For values in the device of $\epsilon_2 < 0$, $-\epsilon_2 > \epsilon_1$ and $-\epsilon_2 > \epsilon_3$, one finally reaches the condition for amplification as

$$-\operatorname{Re}\{\epsilon_2\}(\epsilon_1 + \epsilon_3) \gg 0 \tag{17}$$

which allows an approximately exponential growth of the overall transmission coefficient T_p of the evanescent waves to be realized. For our experiments, $\operatorname{Re}\{\epsilon_2\} \approx -25$, $\epsilon_1 = 1$, $\epsilon_3 = 2.25$, and equation (17) is readily satisfied. Actually, the condition is readily satisfied, considering the experimental situation where the size of the exciting laser is relatively large and thus the wavenumber becomes an almost pure real number.

Therefore, surface waves transmitted to the substrate/silver are amplified with a large enhancement by the silver thin film, which fulfills the condition for the sub-diffraction-limit resolution that was put forward in section 2.

The above theoretical analysis and deduction predicates the possible surface plasmon amplification for thin metallic films. We have carried out additional experiments to confirm the predication of surface plasmon amplification by a thin silver film. We used the same experimental setup and samples as those described in section 3 to have obtain the images presented in figure 3. However, in the new experiments we picked up the signal from the silver side instead of from the substrate side. We present the new experimental results in figure 5. It can be seen clearly that the sub-diffraction-limit pit arrays can also be read out dynamically. Similarly to the situation for readout from the substrate side, the course for readout from the silver side can be described briefly as follows. The surface plasmon waves are excited on the silver/air interface. The surface waves propagating along the silver surface are scattered by the pit trains into propagating waves. The propagating waves are picked up for the readout. Therefore, in the detected signal, the sub-diffraction-limit pit trains are also resolved as shown in figure 5. However, comparing the signal strength in figure 5 with that in figure 3, one finds that the readout signals from the substrate side are significantly larger than those from the silver

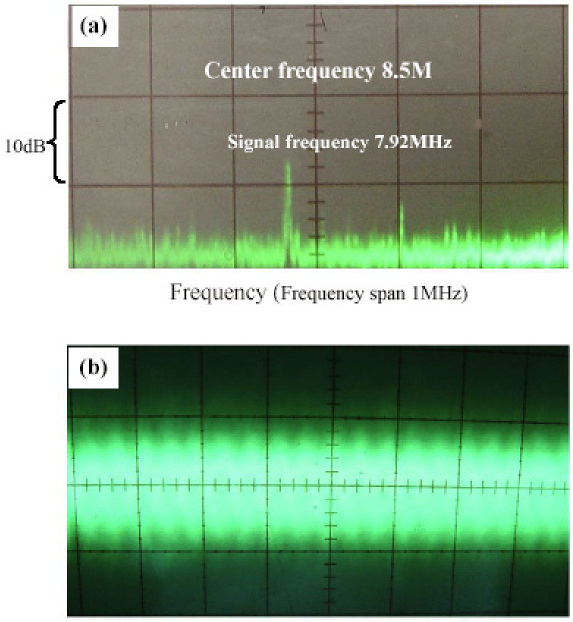

Figure 5. Dynamic readout signal of pit trains from the silver side (linear velocity 6 m s^{-1}): (a) spectral analysis; (b) RF waveform.

side. The carrier-to-noise ratio is about 25 db from the substrate side, as shown in figure 3, and only 15 db from the silver side, as shown in figure 5. This is indeed strong experimental evidence that the surface plasmon waves are amplified and enhanced by the silver thin film.

In passing, we also emphasize that amplification is possible only for ultrathin metallic films, because the condition $r_{12}r_{23} \gg \exp(-2ik_{z2}d)$ would no longer hold for a significant thickness d, and in this case the transmission coefficient remains an exponentially decaying function. Another important consequence of increased thickness d is that the carrier-to-noise ratio would be decreased dramatically due to the optical absorption stemming from the increased film thickness. Reducing the film thickness would not only establish amplified surface plasmon waves, but also diminish the optical absorption, as shown previously in figure 4 of [12].

6. Conclusion

In sections 4 and 5, the key steps that are involved in readout are explored. It is confirmed both theoretically and experimentally that, for our configuration, a strong surface plasmon polariton can be established and amplified by the silver thin film. Since the surface waves bear a spatial wavelength that is shorter than the wavelength of the light, the scattered waves that are collected by the pick-up lens may contain information about the sub-diffraction-limit details of the pit arrays, and thus enable dynamic readout with a sub-diffraction-limit resolution. The above has already been deduced extensively in section 2, and can be summarized as follows.

The sub-diffraction-limited pit arrays can be read out dynamically by the silver thin film. In this course, first, the surface plasmons can be excited at the silver/air interface, then surface plasmon waves are enhanced and amplified by the silver thin film. At the substrate/silver interface, the enhanced surface plasmon waves propagate along the interface. Since the silver thin film is a sinusoidal distribution morphology, the surface waves can be scattered and decoupled into propagating waves by the pit arrays. The propagating waves can be collected by the converging lens and enter the detector, therefore the sub-diffraction-limit pit arrays are read out dynamically.

Acknowledgments

This work is partially supported by the Shanghai Rising Star Program (no. 05QMX1476), the National Natural Science Foundation of China (nos 60507009 and 60490290), Shanghai Key Basic Research Project (no. 06DJ14007), Chinese Academy of Sciences (no. KJCXZ.YW.NANO.06) and UNAM-DGAPA IN120406-3.

References

[1] Pendry J B 2000 *Phys. Rev. Lett.* **85** 3966
[2] Smith D R 2005 *Science* **308** 502
[3] Zhao Z, Fang N, Yen T J and Zhang X 2003 *Appl. Phys. Lett.* **83** 5184
[4] Fang N, Zhao Z, Yen T J and Zhang X 2003 *Opt. Express* **11** 682
[5] Fang N, Lee H, Sun C and Zhang X 2005 *Science* **308** 534
[6] Fang N and Zhang X 2003 *Appl. Phys. Lett.* **82** 161
[7] Melville D O S, Blaikie R J and Wolf C R 2004 *Appl. Phys. Lett.* **84** 4403
[8] Melville D O S and Blaikie R J 2004 *J. Vac. Sci. Technol.* B **22** 3470
[9] Melville D O S and Blaikie R J 2005 *Opt. Express* **13** 2127
[10] Raether H 1988 *Surface Plasmons on Smooth and Rough Surfaces and on Gratings* (New York: Springer)
[11] Veselago V G 1968 *Sov. Phys.—Usp.* **10** 509
[12] Wei J and Gan F 2005 *Appl. Phys. Lett.* **87** 211101
[13] Wei J and Gan F 2002 *Opt. Eng.* **41** 2073
[14] Wei J, Ruan H, Shi H and Gan F 2002 *Chin. Sci. Bull.* **47** 1604
[15] Garcia N and Nieto-Vesperinas M 2002 *Phys. Rev. Lett.* **88** 207403
[16] Li C, Holt J M and Efros A L 2006 *J. Opt. Soc. Am.* B **23** 490 and the references therein
[17] Xiao M 1997 *J. Mod. Opt.* **44** 1609
[18] Chen W and Mills D L 1986 *Phys. Rev.* B **35** 524
[19] Palik E D 1991 *Handbook of Optical Constants of Solids* (San Diego, CA: Academic)
[20] Fang N, Liu Z, Yen T J and Zhang X 2005 *Appl. Phys.* A **80** 1315
[21] Xiao M, Machorro R and Siqueiros J 1998 *J. Vac. Sci. Technol.* A **16** 1420
[22] Keller O, Xiao M and Bozhevolnyi S 1993 *Surf. Sci.* **280** 217